



## How do wettability, zeta potential and hydroxylation degree affect the biological response of biomaterials?



S. Spriano<sup>a,\*</sup>, V. Sarath Chandra<sup>a,b</sup>, A. Cochis<sup>c,d</sup>, F. Uberti<sup>c</sup>, L. Rimondini<sup>c,\*</sup>, E. Bertone<sup>a</sup>, A. Vitale<sup>a</sup>, C. Scolaro<sup>e</sup>, M. Ferrari<sup>f</sup>, F. Cirisano<sup>f</sup>, G. Gautier di Confienzo<sup>g</sup>, S. Ferraris<sup>a,1</sup>

<sup>a</sup> Politecnico di Torino, Department of Applied Science and Technology, Italy

<sup>b</sup> Chosun University, Department of Chemistry, Republic of Korea

<sup>c</sup> Università degli Studi del Piemonte Orientale Amedeo Avogadro, Department of Health Sciences, Novara, Italy

<sup>d</sup> Università degli Studi di Milano, Department of Biomedical, Surgical and Dental Sciences, Milano, Italy

<sup>e</sup> Università degli Studi di Messina, Department of Mathematics and Computer Science, Physics and Earth Sciences, Messina, Italy

<sup>f</sup> Consiglio Nazionale delle Ricerche, Institute for Energetics and Interphases, Genova, Italy

<sup>g</sup> Consiglio Nazionale delle Ricerche, Imamotoer, Torino, Italy

### ARTICLE INFO

#### Article history:

Received 10 October 2016

Received in revised form 19 December 2016

Accepted 20 December 2016

Available online 24 December 2016

#### Keywords:

Wettability

Zeta potential

Hydroxylation

Protein adsorption

Cell adhesion

Bacterial adhesion

Blood wettability

### ABSTRACT

It is well known that composition, electric charge, wettability and roughness of implant surfaces have great influence on their interaction with the biological fluids and tissues, but systematic studies of different materials in the same experimental conditions are still lacking in the scientific literature. The aim of this research is to investigate the correlations between some surface characteristics (wettability, zeta potential and hydroxylation degree) and the biological response (protein adsorption, blood wettability, cell and bacterial adhesion) to some model biomaterials. The resulting knowledge can be applied for the development of future innovative surfaces for implantable biomaterials. Roughness was not considered as a variable because it is a widely explored feature: smooth surfaces prepared by a controlled protocol were compared in order to have no roughness effects. Three oxides (ZrO<sub>2</sub>, Al<sub>2</sub>O<sub>3</sub>, SiO<sub>2</sub>), three metals (316LSS steel, Ti, Nb) and two polymers (corona treated polystyrene for cell culture and untreated polystyrene for bacteria culture), widely used for biomedical applications, were considered. The surfaces were characterized by contact profilometry, SEM-EDS, XPS, FTIR, zeta potential and wettability with different fluids. Protein adsorption, blood wettability, bacterial and cell adhesion were evaluated in order to investigate the correlations between the surface physicochemical properties and biological responses.

From a methodological standpoint, XPS and electrokinetic measurements emerged as the more suitable techniques respectively for the evaluation of hydroxylation degree and surface charge/isoelectric point. Moreover, determination of wettability by blood appeared a specific and crucial test, the results of which are not easily predictable by using other type of tests.

Hydroxylation degree resulted correlated to the wettability by water, but not directly to surface charge. Wetting tests with different media showed the possibility to highlight some differences among look-alike materials. A dependence of protein adsorption on hydroxylation degree, charge and wettability was evidenced and its maximum was registered for surfaces with low wettability in both water based and protein containing media and a moderate surface charge. As far as bacterial adhesion is concerned, no effect of surface charge or protein adsorption was evidenced, while the presence of a high acid component of the surface energy appeared significant. Finally, the combination of hydroxylation degree, wettability, surface charge and energy (polar component) emerged as a key parameter for cell adhesion and viability.

© 2016 Elsevier B.V. All rights reserved.

### 1. Introduction

A thorough knowledge of interaction between the different surface features and biological response to biomaterials is required both for a better understanding of in-vivo behaviour of implants and design of innovative biomaterials and surfaces.

It is qualitatively well known that surface properties (roughness, chemical composition, charge, wettability and hydroxylation degree)

\* Corresponding author at: Politecnico di Torino, Department of Applied Science and Technology, Corso Duca degli Abruzzi, 24, 10129 Turin, Italy.

E-mail address: [silvia.spriano@polito.it](mailto:silvia.spriano@polito.it) (S. Spriano).

<sup>1</sup> Co-shared authorship.

can determine interaction of the biomaterials with the biological environment [1–3] and some general rules are reported in literature [4,5], but they are not proved on a quantitative scale and it is not clear if the same rules apply for materials with different chemical nature (metals, oxides, polymers).

On a time scale, the first contact (during some nanoseconds) is between the implant surface and the water molecules of the biological fluids, then ions are adsorbed, and, after few seconds, proteins cover the surface. Finally, in a time interval typically comprised between some minutes and few hours, different kinds of cells will approach the material, already covered by a protein layer [1]. At the same time, bacteria can compete with the cells for surface colonization: a sort of “race for the surface” has been described between cells and bacteria upon biomaterials implantation in the human body [6]. Surface characteristics, such as topography, chemistry and surface energy, affect the material ability to adsorb water and proteins and consequently to interact with cells and bacteria. Numerous studies have been focused on the effects of surface topography (both at the micro and nanoscale) on cellular and bacterial adhesion [2,3,7–15], that is why it has been decided not to go ahead on this side.

The importance of surface wettability, surface energy and hydroxylation degree on cellular and bacterial adhesion has been highlighted in the scientific literature [16–22], but a more systematic approach is needed. The majority of the cited papers are focused on titanium substrates [23], but the techniques used for the characterization of the surfaces vary from paper to paper and a comparison between the materials investigated by different research groups is difficult. Therefore, a systematic investigation of the effect of the surface characteristics of different biomaterials on their biological response, performed with a coherent experimental protocol, is still lacking.

Eight different substrates (i.e. alumina, silica zirconia, titanium, steel, niobium and treated/untreated polystyrene) have been chosen for this research, according to the following rationale. They are widely employed for biomedical applications (e.g. dental and orthopaedic prostheses), they cover a wide range of materials with different chemistry (metals, oxides and polymers) and crystallographic structure (crystalline, amorphous), they are known to be non-toxic and they show a negligible ion release (at least at short times). That is why they are suitable in order to verify the influence of some surface chemical and physical parameters on the biological response of biomaterials. A protocol for samples surface preparation has been developed in order to obtain comparable roughness and cleaning on all the tested materials, allowing the determination of the effects of the other surface characteristics, on the biological response. In fact, it has already been evidenced that surface properties (e.g. wettability) can vary in a considerable way depending on the sample preparation procedure [16].

Surface chemical composition, hydroxylation degree, wettability by different fluids (i.e. water, Simulated Body Fluid (SBF), Foetal Bovine Serum (FBS), cell culture medium, bacterial culture medium, human

blood and organic solvents), zeta potential, protein adsorption, bacterial adhesion and cell adhesion have been determined for all the selected materials in the present research work. Eventual relationships between the physicochemical surface characteristics of the various substrates and their biological response (blood wettability, protein adsorption, cell adhesion, bacterial adhesion and biofilm formation) are discussed in this paper.

## 2. Materials and methods

### 2.1. Specimens

Eight different materials (Table 1) have been selected for this characterization and samples of comparable area were obtained for each one.

All the oxide and metal samples were mirror polished with SiC abrasive papers (up to 4000 grit); a final polishing suspension (OP-U suspension, Struers, SiO<sub>2</sub> 0.04 μm) was used on metals in order to obtain uniform and comparable surfaces. Roughness measurements, obtained by contact profilometry, are reported in Table 2.

In order to obtain clean and comparable surfaces for analyses, the oxide and metal samples were washed in an ultrasonic bath for 5 min in acetone and subsequently two times in ultrapure water for 10 min. At the end of the washing steps, samples were dried in a laminar flow cabinet (FASTER CYTOSAFE-N 2000) and decontaminated with UV irradiation for 1 h under the same cabinet. Samples were then packed in aluminium foils and closed in plastic-paper bags for sterilization until use.

Polystyrene substrates for cells and bacteria cultures were used without carrying on any further surface modifications or cleaning, their roughness is reported in Table 2 as well.

### 2.2. Characterization

In order to investigate surface topography and cellular shape after cell culture tests, samples were observed by means of Scanning Electron Microscopy equipped with Energy Dispersive Spectroscopy for chemical analyses (SEM – FEI, QUANTA INSPECT 200, EDS – EDAX PV 9900). The oxide samples were sputter coated with a thin Cr layer (5–10 nm) before observation.

Surface chemical composition and hydroxylation degree were evaluated by means of XPS analyses (XPS, PHI 5000 VERSA PROBE, PHYSICAL ELECTRONICS). Both the survey spectra and the high resolution spectra of carbon and oxygen regions were acquired. All the high resolution spectra were referenced by setting the hydrocarbon C1s peak to 284.80 eV for charging effect compensation.

Fourier Transformed InfraRed Spectroscopy (FTIR) (FT-IR, IR Hyperion 2000, Alpha, Bruker Optics) measurements were performed for a further characterization of surface chemical composition and hydroxylation

**Table 1**  
Materials.

Material	Symbol	Class	Surface treatment	Structure	Source
Silica	SiO <sub>2</sub>	Oxide	–	Amorphous	Heraeus HSQ300
Alumina	Al <sub>2</sub> O <sub>3</sub>	Oxide	–	Crystalline: gamma	Expert System Solutions S.r.l.
Zirconia	ZrO <sub>2</sub>	Oxide	–	Crystalline: cubic and tetragonal, TZP-A (95% ZrO <sub>2</sub> , 5% Y <sub>2</sub> O <sub>3</sub> , 0.25% Al <sub>2</sub> O <sub>3</sub> )	Metoxit
Titanium	Ti-commercially pure grade 2	Metal (pure)	–	Crystalline: hexagonal	Titanium Consulting and Trading
Niobium	Nb	Metal (pure)	–	Crystalline: body centred cubic	New Tech
Steel	316L	Metal (alloy)	–	Crystalline: face centred cubic	Tresoldi Metalli
Polystyrene for cells culture	PS-cells	Polymer	CORONA treatment for eukaryotic cells culture	Amorphous	Nunclon Delta Surface, Thermo Fisher Scientific, Roskilde, Denmark
Polystyrene for bacteria cultures	PS-bact	Polymer	–	Amorphous	Sterilin, PBI-VWR International, Milan, Italy

**Table 2**  
Roughness measurements (Ra mean  $\pm$  standard deviation).

Sample	Roughness [ $\mu\text{m}$ ]
Silica	0.016 $\pm$ 0.001
Alumina	0.031 $\pm$ 0.006
Zirconia	0.041 $\pm$ 0.021
Titanium	0.015 $\pm$ 0.004
Niobium	0.013 $\pm$ 0.001
Steel	0.007 $\pm$ 0.001
PS-cells	0.009 $\pm$ 0.000
PS-bact	0.008 $\pm$ 0.001

degree. The spectra were recorded from 4000 to 600  $\text{cm}^{-1}$  in reflection mode.

Static contact angles were measured by the sessile drop method. A drop (5  $\mu\text{l}$ ) of different fluids (listed below) was deposited on the sample surface and its shape recorded by a camera (Misura®, Expert System Solutions) under atmospheric condition at room temperature and standard deviation due to experimental error was calculated as  $\pm 1^\circ$ . The contact angle was determined by Image J software (1.47 version).

The fluids considered in the present research work were: Simulated Body Fluid (SBF, prepared according to the protocol proposed by Kokubo) [24], Foetal Bovine Serum (commercial, FBS, Sigma-Aldrich, Milan, Italy), cell culture medium (commercial, Dulbecco's Modified Eagle Medium, DMEM, Sigma-Aldrich, Milan, Italy), bacterial culture broth (commercial, Luria Bertani, LB, Sigma-Aldrich, Milan, Italy).

Blood considered for this experiment is human blood taken from a healthy volunteer. The blood samples were taken in a laboratory of clinical analysis and stored in a refrigerator (2–6  $^\circ\text{C}$ ), in their original sterile tubes (BD Vacutainer K3E, with 5.4 mg ethylenediaminetetraacetic acid - EDTA). EDTA binds calcium ions, thus inhibiting the coagulation cascade. The measurements of the contact angles were performed on the different samples within 5 days from the donation, in order to save blood from possible deterioration. The approximate haemochrome cytometric values for blood counts are reported in Table 3.

The measurement of the contact angle of blood on the different surfaces was performed by the sessile drop method [25,26].

A calibrated syringe (Hamilton 10  $\mu\text{l}$ ) was used to deposit the blood drops. Before the contact angle measurement, the tube containing the blood sample was shaken to homogenise the content till blood temperature reached room temperature. The temperature measurements for this study were obtained using Sika Electronic digital thermometer (TS 9180). The drops of blood (1  $\mu\text{l}$ ) were gently placed by the calibrate syringe on the samples ( $T = 22^\circ\text{C}$ ,  $\text{RH} = 35\%$ , and  $P = 1\text{ atm}$ ) in a perfectly horizontal position. Six measurements of contact angle were performed on the drops of blood placed at different points of each sample

**Table 3**  
Haemochrome cytometric values for blood.

Blood group	A1 Rh positive, phenotype Rh e Kell, CcDEe kk
Haemochrome	White blood cells (WB) = $6.7 \times 10^3/\text{ml}$ , neutrophils (N) = 66.2%, lymphocytes (l) = 25.1%, monocytes (M) = 7.9%, eosinophils (E) = 0.5%, basophils (B) = 0.3% Red blood cells (RB) = $4.16 \times 10^6/\mu\text{l}$ , haemoglobin (Hb) = 13.4 g/dl, haematocrit (Ht) = 39.3%, Mean Corpuscular Volume (MCV) = 94.5 fl, Mean Corpuscular Haemoglobin (MCH) = 32.3 pg, Mean Corpuscular Haemoglobin Concentration (MCHC) = 34.2% Platelets = $214 \times 10^3/\mu\text{l}$ , Mean Platelet Volume (MPV) = 8.1 fl, procalcitonin (PCT) = 0.173%, Platelet Distribution Width (PDW) = 17.5 fl
Coagulation	Prothrombin activity INRI = 0.9; activated Partial Thromboplastin Time Ratio (aPTT R) = 0.86, fibrinogen = 380 mg/dl
Biochemistry	Blood glucose = 91 mg/dl, creatinine = 0.7 mg/dl, homocysteine = 11.2 $\mu\text{mol/l}$
Specific proteins	Albumin = 36 g/l, protein C = 76%, total protein S = 58%

and the average contact angle value was subsequently determined. Reproducibility of the contact angle readings is  $\pm 2^\circ$ .

The surface tension measurements were performed by the method of the dropper. The measurements were carried out at room temperature and humidity ( $T = 22^\circ\text{C}$ , U.R. = 35%), by slowly dripping blood from a dropper of radius equal to 1.2 mm on an electronic balance (Kern KB 120-3 N, max 121 g,  $d = 0.001\text{ g}$ ). The measurement of the weight of 15 drops was performed and averaged (1 drop of blood is approximately 0.047 g).

Theoretical viscosity of blood as a function of haematocrit was calculated using the formula of Bull:

$$\mu_s = \mu_p(1 + 2.5Ht)$$

where  $\mu_p$  indicates the density of plasma and Ht is haematocrit. The experimental measurements of viscosity were performed by measuring the rate of outflow of the fluid from a capillary of known volume. Ten independent measurements were taken and averaged.

For the evaluation of the surface energy of the samples, contact angle (CA) measurements were carried out by the ASTRAview tensiometer (developed at CNR-IENI [27]) at room temperature (22  $^\circ\text{C}$ ). In order to assess the homogeneous character of the film deposition the data were collected in at least 3 different positions of the surface

The following fluids were used: High purity grade water, produced by a MilliQ (Milli-Pore) ion-exchange purifier with a microfiltration stage, Trichloromethane (commercial, CHROMASOLV® Plus, for HPLC,  $\geq 99.9\%$ , Sigma-Aldrich, Milan, Italy), 2-Butanone (CHROMASOLV® Plus, for HPLC,  $\geq 99.7\%$ , Sigma-Aldrich, Milan, Italy, BUT), decane (ReagentPlus®,  $\geq 99\%$ , Sigma-Aldrich, Milan, Italy, DEC)

Three different approaches were considered for determination of the isoelectric point of the selected materials: one liquid contact angle titration, two liquids contact angle titration and electrokinetic measurement.

The first two methods foresee measurement of the contact angles of aqueous solutions with different pH on the solid surface. As the contact angle is maximum (and cosine is minimum) at the isoelectric point (IEP), IEP can be determined by the trend of the contact angle values vs pH [28,29]. The contact angle measurements were performed in air (one liquid method) or in a liquid immiscible with water (two liquids contact angle titration) in order to improve accuracy and repeatability of the test [28,29]. A FTA 1000C instrument was used for both the methods. 2 M NaCl was used as an electrolyte for the aqueous solutions at different pH. The pH value was adjusted by addition of 0.001 M NaOH or 0.002 M HCl: 0.5 pH intervals were considered. Hexadecane (anhydrous  $\geq 99\%$ , Sigma Aldrich) was employed as a second liquid for the two-liquids contact angle titration.

As far as the electrokinetic measurements are concerned, the model of the electrochemical double layer for definition of zeta potential has been considered. In this model zeta potential is defined as the electrical potential at the shear plane and the shear plane is defined as the boundary between stationary and diffuse layers of charges at the solid-liquid interface [30]. Zeta potential of solid surfaces was determined by the measurement of an electrokinetic effect (streaming potential/current) due to the relative movement of solid-liquid phases. An electrokinetic analyser (SurPASS, Anton Paar) equipped with an adjustable gap cell was employed for the measurements. 0.001 M KCl was used as an electrolyte and its pH was adjusted by the addition of 0.05 M HCl or 0.05 M NaOH by means of the instrument automatic titration unit.

### 2.3. Protein amount quantification

Three disks of the different materials were incubated in FBS for 1 h at 37  $^\circ\text{C}$  in order to determine the different adsorption capacity of the samples and the total amount of adsorbed proteins was quantified by the bicinchoninic acid assay (BCA, Sigma-Aldrich) [31]. After incubation in FBS, the proteins adsorbed on the sample surface were lysed in 50  $\mu\text{l}$

of Ripa Buffer (50 mM Hepes, 150 mM NaCl, 0.1% SDS, 1% Triton-X100, 1% sodium deoxycholate, 10% glycerol, 1.5 mM MgCl<sub>2</sub>, 1 mM EGTA, 1 mM NaF) and gently collected using a cell scraper. To determine the weight ( $\mu\text{g}$ ) of protein on each sample, a standard curve was generated using bovine serum albumin (BSA, Sigma, 0–5  $\mu\text{g}$ ) and mixed with BCA kit reagents. The absorbance value of all samples and the standard curve was measured at 570 nm by a spectrometer (SpectraCount, Packard Bell, USA) and the protein amount calculated as a function of the standard curve.

#### 2.4. Western blot analysis

After quantification, 40  $\mu\text{g}$  of proteins for each sample was dissolved in Laemmli buffer 5 $\times$  (62.5 mM Tris-HCl, pH 6.8, 25% glycerol, 2% SDS, 0.01% Bromophenol Blue), heated at 95 °C for 5 min, resolved on 8% SDS-PAGE and transferred to a PVDF membrane. Finally, the membrane was marked by Coomassie blue and analysed with Image J software (NIH) for protein quantification.

#### 2.5. Bacterial adhesion studies

The exponentially-growing biofilm forming *Staphylococcus aureus* pathogen (clinical isolate from the Hospital Maggiore of Novara) was used to study bacterial adhesion on the test materials. Bacteria were cultivated on LB-agar Petri dishes for 24 h until single round colonies were obtained. Then, single colonies were collected and used to prepare a suspension of LB broth containing  $1 \times 10^7$  cells/ml, according to McFarland 1.0 standard optical density. The Petri dishes were stored at 4 °C while fresh broth culture prepared prior to each experiment.

#### 2.6. *Staphylococcus aureus* biofilm adhesion

The specimens were sterilized by 2 h through immersion in 70% ethanol and UV light exposure (30 min) prior to use. Then, the samples were singularly placed into the wells of a 24 multi-well plate (Nunc Delta Surface, Thermo Fisher Scientific); then, 1 ml of the bacterial prepared suspension was used to fill the wells containing the specimens. The plate was incubated for 90 min at 37 °C in a humid atmosphere in agitation (120 rpm, adhesion phase) [32,33]. Afterwards, the plate was collected and the supernatants were removed in order to discard the floating planktonic cells and cultivate the biofilm cells attached on the specimen surface. The wells were then rinsed with 1 ml of fresh LB medium and cultivated for 24 h at 37 °C (biofilm cultivation phase) [32,33].

#### 2.7. Colonies forming units (CFUs) count

After 24 h of cultivation, the specimens were collected, washed with phosphate buffered saline (PBS, pH 7.4, Sigma) and stored in 15 ml falcon tubes containing 1 ml of PBS. The tubes were sonicated (Ultrasonic 250, PBI) and vortexed (5 times each, 30 s) in order to detach the biofilm cells from the surface. Afterwards, 200  $\mu\text{l}$  were collected from the tubes and used to perform 6 tenfold serial dilutions; 20  $\mu\text{l}$  of each dilution were spotted into Mannitol Salt agar plates previously divided into 6 cloves. Bacteria final number was calculated using the following formula: [(number of single colonies)<sup>^</sup>(reverse of tenfold dilution)  $\times$  dilution factor] [32,33].

#### 2.8. Bacteria metabolic activity

*S. aureus* biofilm metabolic activity was evaluated by the colorimetric 2,3-bis (2-methoxy-4-nitro-5-sulphophenyl)-5-[(phenyl amino) carbonyl]-2H-tetrazolium hydroxide (XTT, Sigma) assay. After 24 h of cultivation, the specimens were collected, washed with PBS and placed into a new 24 multi-well plate. Each well was filled with 1 ml of fresh medium (LB) and supplemented with 100  $\mu\text{l}$  of XTT solution (3 mg/ml

in PBS containing 1 mM menadione). The plate was incubated 5 h in the dark; afterwards, the supernatants were collected and centrifuged (12,000 rpm) in order to remove eventual debris. From each sample, 100  $\mu\text{l}$  were collected and spotted into a 96 multi-well plate; sample optical density was evaluated at 490 nm by a spectrophotometer (SpectraCount, Packard Bell, Chicago, USA) [32,33].

#### 2.9. Human Cells adhesion evaluation

Human foetal osteoblasts (hFOB 1.19, ATCC CRL-11372, purchased from the American Type Culture Collection) were cultivated in MEM:HAM'S F12 mixture (Sigma) supplemented with 0.3 mg/ml G418 salt (Sigma), 10% Foetal Bovine Serum (FBS, Sigma) and 1% antibiotics at 34 °C, in humid atmosphere with 5% CO<sub>2</sub>. The cells were cultivated until 80–90% confluence, detached with trypsin-EDTA (0.05% in PBS, Sigma) and used for the experiments.

The specimens were sterilized by ethanol immersion (70% ethanol, 2 h) and located into the wells of a 24 plate (Nunc Delta). The cells were collected and seeded in a defined number ( $1.5 \times 10^4$  cells) in 500  $\mu\text{l}$  of media, used to submerge the specimens. The plate was incubated at 34 °C, 5% CO<sub>2</sub> for 24 h; afterwards, cells viability was evaluated by the colorimetric 3-(4,5-dimethylthiazol-2-yl)-2,5-diphenyltetrazolium bromide (MTT) assay (Sigma). An aliquot of 100  $\mu\text{l}$  of MTT solution (3 mg/ml in PBS) was added to each well and stored for 4 h at 34 °C in the dark; afterwards, the supernatants were removed and the formazan crystals solved by adding 100  $\mu\text{l}$  of DMSO/well. Then, an aliquot of 50  $\mu\text{l}$  was collected from each well, centrifuged (12,000 rpm, 5 min) to remove debris and finally spotted into a new 96 wells plate. Sample optical density (o.d.) was measured with a spectrophotometer (SpectraCount, Packard Bell) at 570 nm. The cells cultivated into the polystyrene wells were used as a positive control (group a) and considered as 100% viability while the test samples results were expressed as a function of controls. On the other hand not-treated polystyrene (for bacteria) was considered as a negative control (group c). Experiments were performed in quadruplicate.

Finally, the morphology and the spread of cells cultivated onto materials of interest (Group b) were compared by means of SEM.

#### 2.10. Statistical analysis of the data

Statistical analysis of physicochemical and biological data was performed through ANOVA one way tests (significance level increasing from  $p < 0.05$  to  $p < 0.01$  and  $p < 0.001$ ). Finally, the Scheffé's post hoc multiple comparison tests were performed to detect significant differences between groups.

### 3. Results

Eight different substrates have been chosen for this research, in order to verify the influence of some chemical and physical surface parameters (isoelectric point, hydroxylation degree, surface energy and wettability), on the biological response (blood wettability, protein adsorption, cell adhesion, bacterial adhesion and biofilm formation) on a wide range of materials (metals, polymers and oxides) employed for biomedical applications.

A polishing procedure was optimized for each material in order to get smooth surfaces with comparable roughness and to avoid effects due to the different surface morphology of the materials, which is not the aim of the present work. The surface morphology was controlled by SEM observations (not reported) and roughness measurements (see Table 1).

#### 3.1. Chemical analyses

The chemical composition of the selected surfaces was analysed by means of EDS, XPS and FTIR.



No relevant surface contamination was detected by EDS, in the limits of 0.1 wt%, on any of the examined surfaces.

No relevant contamination was found on the tested materials, apart from unavoidable carbon content, through XPS analysis. XPS measurements on PS substrates were not performed because gas emission from these materials in high vacuum condition was too high. Literature data can be used as reference [34–36], where corona treated Polystyrene for cell culture shows an enhanced density of hydroxyl and carboxyl functional groups of about 10% with respect to the untreated one.

The high resolution XPS spectra of the oxygen region of the analysed materials are reported in Fig. 1. Attention was focused on hydroxylation degree. The different contributions detected in the high resolution spectra of oxygen have been attributed to the oxygen ions within bulk oxide or within exposed hydroxyl groups, according to the literature data [37–43]. The quantitative ratio between the signal of the OH group and that one of the  $O^{2-}$  ions is reported in Table 4. It was obtained by the ratio between the areas of the corresponding signals in the high resolution spectra of the oxygen region. It can be noted that 316 L stainless steel and silica show the highest hydroxylation degree, titanium and alumina the lowest ones and zirconia and niobium are in a middle position.

Fig. 2 shows the FTIR spectra of the different materials investigated in this work. It is difficult to perform an accurate assignment of the bands in the acquired spectra, obtained by using the reflectance mode, due to the high complexity of the signals.

**Table 4**

Hydroxylation degree from XPS analyses.

Material	OH/ $O^{2-}$
Alumina	0.3
Silica	2.5
Zirconia	0.6
Titanium	0.2
Niobium	0.6
Steel	3.8

The small band at  $2360\text{ cm}^{-1}$  that appears in all the spectra is due to atmospheric  $CO_2$ .

In the spectra registered on the metals (titanium, niobium and steel), the bands related to the stretching vibrations of molecular water and hydroxyl groups (at about  $3500\text{--}3600\text{ cm}^{-1}$ ) [44–46] were observed, together with the bending vibrations of water molecules (at about  $1630\text{ cm}^{-1}$ ). In the case of steel, the OH contribution at  $3500\text{--}3600\text{ cm}^{-1}$  is higher in comparison to the other metals [47].

The characteristic bands of the Nb—O bond are in the range  $600\text{--}1000\text{ cm}^{-1}$  [48]; the peaks at approximately  $640\text{ cm}^{-1}$  and  $680\text{ cm}^{-1}$  in the reported spectrum of niobium can be assigned to niobium pentoxide, that is the native surface oxide layer formed on the metal surface.

In the spectrum of titanium, bands due to the Ti—O bond vibrations were observed in the range of  $600\text{--}640\text{ cm}^{-1}$ .

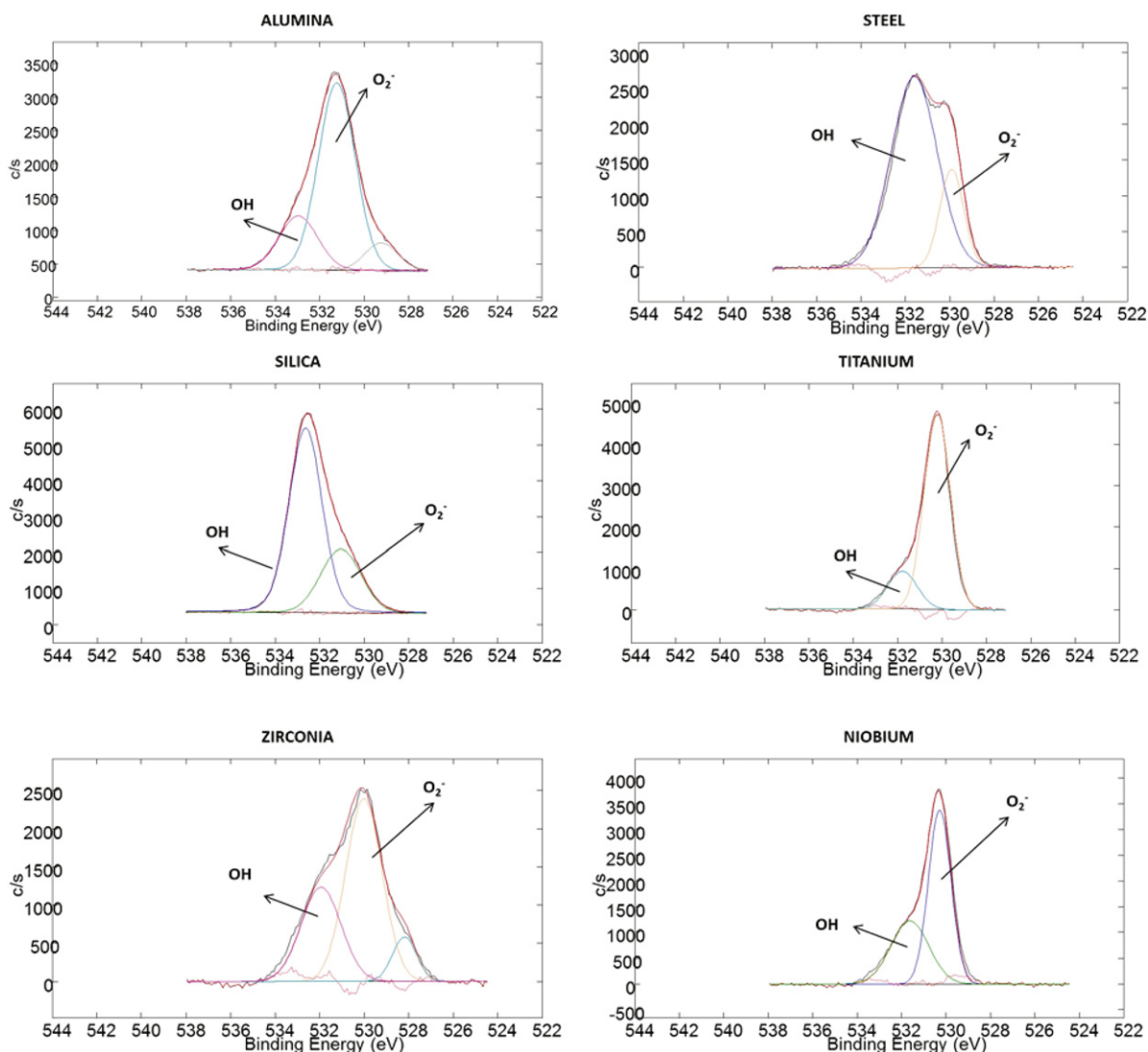


**Fig. 1.** XPS high resolution spectra of the considered materials.

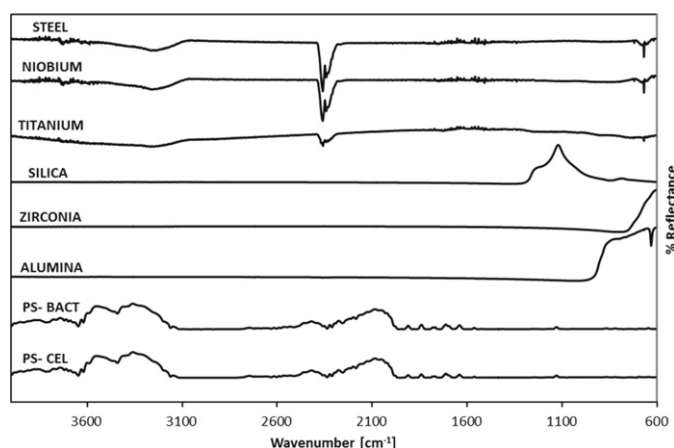


Fig. 2. FTIR spectra of the considered materials.

The spectrum of silica shows three peaks in the range between 1400 and 600  $\text{cm}^{-1}$ , which belong to Si—O bending vibration modes. At 3500–3600  $\text{cm}^{-1}$ , the peaks due to overtones and combinations of vibrations of Si—OH are reported in the literature [49], in addition to the contribution of molecular water, and in the region between 3000 and 1400  $\text{cm}^{-1}$  overtones and combinations of vibrations of  $\text{SiO}_2$  network signals are also reported, but these peaks were not observed on the material tested in this work.

In the spectrum of zirconia, a characteristic peak at around 600  $\text{cm}^{-1}$  can be assigned to  $\text{ZrO}_2$ , according to [50], where the same peak with a maximum at 524  $\text{cm}^{-1}$  is reported.

The spectrum of alumina shows one group of signals related to the stretching vibrations of Al—O bond in the octahedrally coordinated aluminium ions (600–750  $\text{cm}^{-1}$ ), while the bands in the range of 750–900  $\text{cm}^{-1}$  can be assigned to the vibrations of Al—O bond in  $\text{AlO}_4$  units.

Concerning polystyrene for cells and bacteria culture, no difference can be registered by this technique. The contribution of aromatic rings and OH groups can be observed in the spectral range between 3000 and 4000  $\text{cm}^{-1}$ . The aromatic C—H out of plane bending vibrations is observed at 1730–1950  $\text{cm}^{-1}$ . At 1600, 1500 and 1410  $\text{cm}^{-1}$  the aromatic —C=C— stretching vibrations are detected. Aromatic =C—H in-plane deformation vibrations were observed at 1200–1130  $\text{cm}^{-1}$ . At 840–860 and 760  $\text{cm}^{-1}$  aromatic =C—H out-of-plane deformation vibrations can be seen, even if it is a quite weak signal, as at 701  $\text{cm}^{-1}$  out-of- plane ring deformation vibration. Aromatic =C—H stretching vibrations can be seen at 3100  $\text{cm}^{-1}$ , as at 2920  $\text{cm}^{-1}$  alkyl C—H stretching vibrations were not observed [51].

### 3.2. Wettability

The surface tension data of the different liquids used for the measurement of surface energy are summarized in Table 5. These liquids were chosen for their specific component, dispersive, acid, basic, required to measure the surface energy by the van Oss theory (Table 6). In particular, decane was chosen because it has only a dispersive component to its surface tension, Trichloromethane was chosen for its acid component and 2-Butanone for its basic component.

Moreover, the available data of surface tension of the liquids used for the wettability tests are reported in Table 5. SBF and cell culture medium have a surface tension close to pure water while blood, FBS and bacterial culture broth show slightly lower values.

Fig. 3 reports the contact angles values of the different fluids on the considered materials grouped as: inorganic liquids (pure water and SBF – Fig. 3a), organic solvents (Trichloromethane, 2-Butanone and decane – Fig. 3b), biologic fluids without cellular components (FBS, bacterial and cell culture media – Fig. 3c) and blood (Fig. 3d).

Table 5  
Physical properties at  $T = 22\text{ }^\circ\text{C}$  [52–61].

Liquid	Surface tension [mJ/m <sup>2</sup> ]	Dispersive component [mJ/m <sup>2</sup> ]	Acid component [mJ/m <sup>2</sup> ]	Basic component [mJ/m <sup>2</sup> ]
Pure water	72.8	26.4	23.2	23.2
Trichloromethane	27.2	27.2	0	0
2-Butanone (BUT)	24.6	24.60	0	24.0
Decane (DEC)	23.8	23.8	0	0
SBF	72.5	–	–	–
Cell cult. medium	70	–	–	–
FBS	52	–	–	–
Bact. cult. broth	57–60	–	–	–
Whole blood	61	–	–	–

A statistical analysis of each dataset obtained by using the same liquid was performed and briefly summarized below and in Fig. 3.

Concerning the measurements with SBF as a testing liquid, we can divide the tested surfaces in four groups (Fig. 3a), with decreasing contact angle values and no statistically significant difference within each group:

- PS-bact and alumina (group a);
- zirconia and steel (group b);
- titanium and niobium (group c);
- PS-cells and silica (group d).

Statistical differences at a significance level  $p < 0.01$  were found among groups a, c and d (Fig. 3a), while group b is in mid-position without any significant difference in comparison to the other groups.

Concerning the measurements with pure water as a testing liquid (Fig. 3a), the tested surfaces can be divided in five groups:

- PS-bact and alumina (group a')
- PS-cells (group b')
- Zirconia and niobium (group c')
- steel (group d')
- titanium and silica (group e').

The surfaces in group a' show comparable values of contact angle, which are statistically higher than the ones of (reported in decreasing order) groups b' ( $p < 0.05$ ), e' ( $p < 0.01$ ) and d' ( $p < 0.01$ ). Zirconia and niobium (group c') are in a mid-position without any statistical difference in comparison to the other groups.

Concerning the measurements with organic solvents as testing liquids, wettability on polystyrene substrates was not measured because of their great reactivity with the substrate. Butanone completely wets all the surfaces (the contact angle was near  $0^\circ$  and not measurable; it was reported equal to  $1^\circ$ ) except steel, while decane completely wets

Table 6  
Surface energy values for the investigated materials.

	Surface energy [mJ/m <sup>2</sup> ]	Dispersive component [mJ/m <sup>2</sup> ]	Acid component [mJ/m <sup>2</sup> ]	Basic component [mJ/m <sup>2</sup> ]	Polar component [mJ/m <sup>2</sup> ]
Alumina	24.04	23.80	0.01	1.45	0.24
Silica	23.96	23.73	0.01	1.29	0.23
Zirconia	24.00	23.80	0.01	0.96	0.20
Titanium	23.99	23.80	0.01	0.91	0.19
Niobium	23.98	23.80	0.01	0.80	0.18
Steel	23.80	23.80	0.00	1.01	0.00
PS-cells [55]	43.58	38.90	0.40	13.70	4.68
PS-bact [56–58]	46.32	44.31	0.46	2.20	2.01

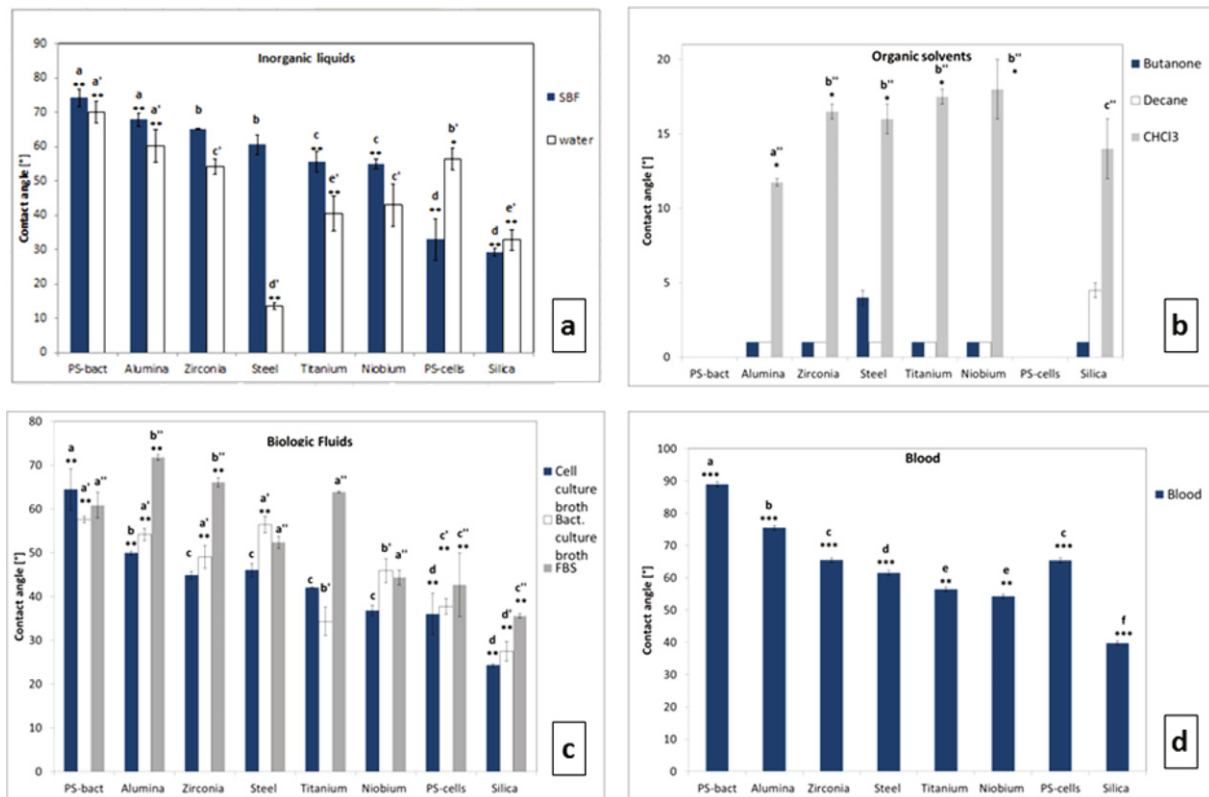


Fig. 3. Static contact angles of different fluids on the considered materials.

all the surfaces except silica. Higher contact angles were measured by using Trichloromethane, the surfaces can be grouped as (Fig. 3b):

- alumina (group a'')
- zirconia, steel, titanium and niobium (group b'')
- silica (group c'').

Group b'' shows contact angle values significantly higher ( $p < 0.05$ ) than group a''; while group c'' has no statistically significant difference in comparison to the other groups.

Concerning the measurements with biological fluids as testing liquids (Fig. 3c), different observations can be done for each fluid.

In the case of the cell culture medium, the surfaces can be grouped as (Fig. 3c):

- PS-bact (group a)
- alumina (group b)
- zirconia, steel, titanium and niobium (group c)
- PS-cells and silica (group d).

No significant differences can be evidenced in group d, which has contact angle values lower than group b (significance level  $p < 0.01$ ), which in turn has contact angle values lower than group a (significance level  $p < 0.01$ ); group c is in a mid-position and it is not statistically different in comparison to the other groups.

In the case of the medium for bacterial culture, the surfaces can be grouped as (Fig. 3c):

- PS-bact, alumina, zirconia and steel (group a')
- titanium and niobium (group b')
- PS-cells (group c')
- silica (group d').

No statistically significant differences can be evidenced in group a' while it has higher contact angle values than groups c' and d'

(significance level  $p < 0.01$ ); group b' is in a mid-position and it is not statistically different in comparison to the other groups.

In the case of FBS, the surfaces can be divided in three groups (Fig. 3c):

- PS-bact, steel, titanium (group a'')
- alumina and zirconia (group b'')
- silica and PS-cells (group c'').

There is a statistically significant difference (at a significance level  $p < 0.01$ ) between group b'' (high contact angle values) and group c'' (low contact angle values), while the other surfaces (group a'') do not show significant differences in comparison to the other tested samples and are in a mid-position.

Concerning the measurements with blood as a testing liquid (Fig. 3d), the surfaces can be grouped as:

- PS-bact (group a)
- Alumina (group b)
- Zirconia and PS-cells (group c)
- Steel (group d)
- Titanium and niobium (group e)
- Silica (group f).

No statistically significant differences can be evidenced in group e as well as in group c, while all the other comparisons give highly significant differences ( $p < 0.01$  or  $p < 0.001$ ). The contact angle values decrease from PS-bact, to alumina, zirconia/PS-cells, steel, titanium/niobium and silica.

All these statistical comparisons were used for a meta-analysis of the data reported in the discussion (Table 7).

At an overview of the results, it appears that the tested materials are almost arranged in the same order of the measured contact angle values, regardless the use of different liquids (water, SBF, cell and

**Table 7**

Meta-analysis of the data: a scale from 1 (minimum value obtained on that test) up to 6 was used in order to compare the features of the investigated materials.

	OH	Wettability									Surf energy			Zeta pot.	IEP pH	BCA	CFU	XTT	Cell Viab.
		H <sub>2</sub> O	SBF	Cell broth	Bact broth	FBS	Blood	BUT	DEC	CHCl <sub>3</sub>	Disp.	Acid	Basic						
Al <sub>2</sub> O <sub>3</sub>	1	1	1	3	1	1	2	6	6	6	4	1	1	3–4	3–4	6	4–5	1	5
SiO <sub>2</sub>	4	4	6	6	6	6	6	6	2	4	4	1	1	1	3–4	1	5	1	5
ZrO <sub>2</sub>	2	3	2	4	1	1	3	6	6	3	4	1	1	3–4	3–4	4	5	1	5
Ti	1	4	4	4	3–4	2–5	5	6	6	3	4	1	1	3–4	4–5	4	5	1	5
Nb	2	3	4	4	3–4	2–5	5	6	6	3	4	1	1	3–4	3–4	4	5	1	5
AlSi316L	6	6	2	4	1	2–5	4	2	6	3	4	1	1	3–4	4–5	4	5	1	5
PS bact	≈1*	1	1	1	1	2–5	1	–	–	–	6	6	6	3–4	3–4	4	6	6	1
PS cell	≈2*	2	6	6	5	6	3	–	–	–	6	6	1–2	6	2–3	4	6	6	6

\*Semi-quantitative data from literature

bacteria culture media, blood). Despite the liquid used for the test, silica is the more wettable surface in most cases (except water), while alumina and polystyrene for bacterial cultures are the less wettable ones. Polystyrene for cell cultures generally has low contact angles with all the investigated fluids (slightly higher with blood). Zirconia, steel, titanium and niobium generally have mid-range values of contact angle among the explored materials. Titanium and niobium show quite similar wettability. The use of different liquids is useful in order to evidence differences between similar surfaces, such as alumina and PS-bact which are differently wetted by cell culture medium and FBS.

In general, the highest contact angle values have been obtained using blood as wetting fluid, on most of the tested materials, while the lowest contact angle values were obtained by using bacterial and cell culture media (except on steel).

Surface energy values were obtained for the different materials, as reported in Table 6. In the case of polystyrene for bacteria and cells cultures, the measurements were not experimentally performed in this research because of the high reactivity of the polymer with the liquids used for the tests. The literature data are reported in this case.

It is possible to observe that many materials show the same value of dispersive components (around 24 mJ/m<sup>2</sup>) and of the acid component (around 0.01 mJ/m<sup>2</sup>). This is in agreement with the van Oss model [56] because only the decane contact angle values were taken into account to predict the dispersive component and the contact angle was considered 1° on all the surfaces (slightly different for silica), because the liquid completely wets the surfaces. The same reason is valid for calculation of the acid component: decane and 2-Butanone completely wet all the surfaces (slightly different for steel).

Polymers, as expected, show complete different values, with higher dispersive and polar components. PS-cells shows a greater Basic component than PS-bact.

### 3.3. Isoelectric point and zeta potential

The isoelectric point was measured for each material by means of both contact angle titration (with one or two liquids) and the electrokinetic technique.

Although the contact angle measurements as a function of pH have been proved useful in the literature for the assessment of the isoelectric point of flat metal substrates, this method failed to give reliable results in our case due to excessive data dispersion. An example of the obtained

graphs is reported in Fig. 4 for alumina, respectively tested by the method of one (Fig. 4a) and two liquids (Fig. 4b) contact angle titration. This method cannot be considered reliable for the purposes of this work.

Zeta potential in function of the pH value of the test solution and IEP, measured by means of the electrokinetic technique, is reported in Fig. 5 for the considered materials. The IEP can be measured as the intercept of the curve with the abscissa axis. Three measures were performed on each type of material, but only one measurement is reported in Fig. 5 for better clarity; average IEP values and zeta potential at physiologic pH were calculated for the three measures performed on each material

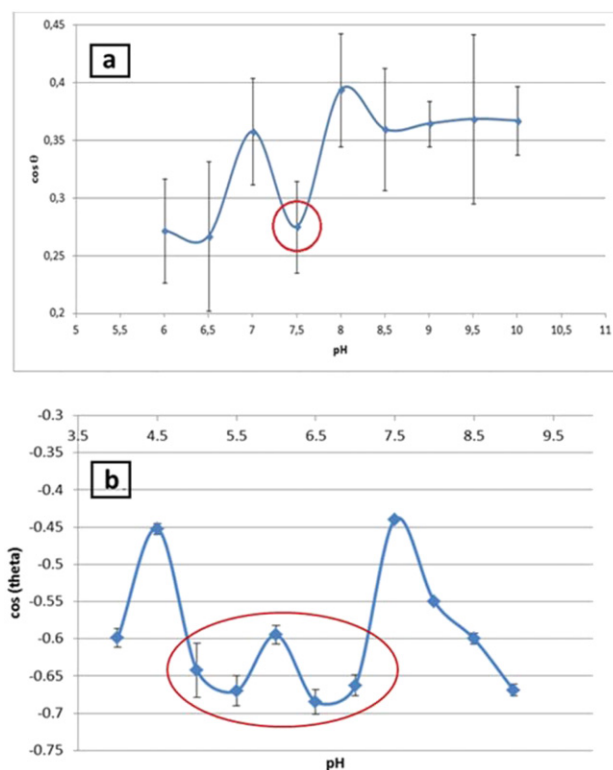


**Fig. 4.** Isoelectric point determination by contact angle titration method for alumina samples. a) One liquid, b) two liquids method.



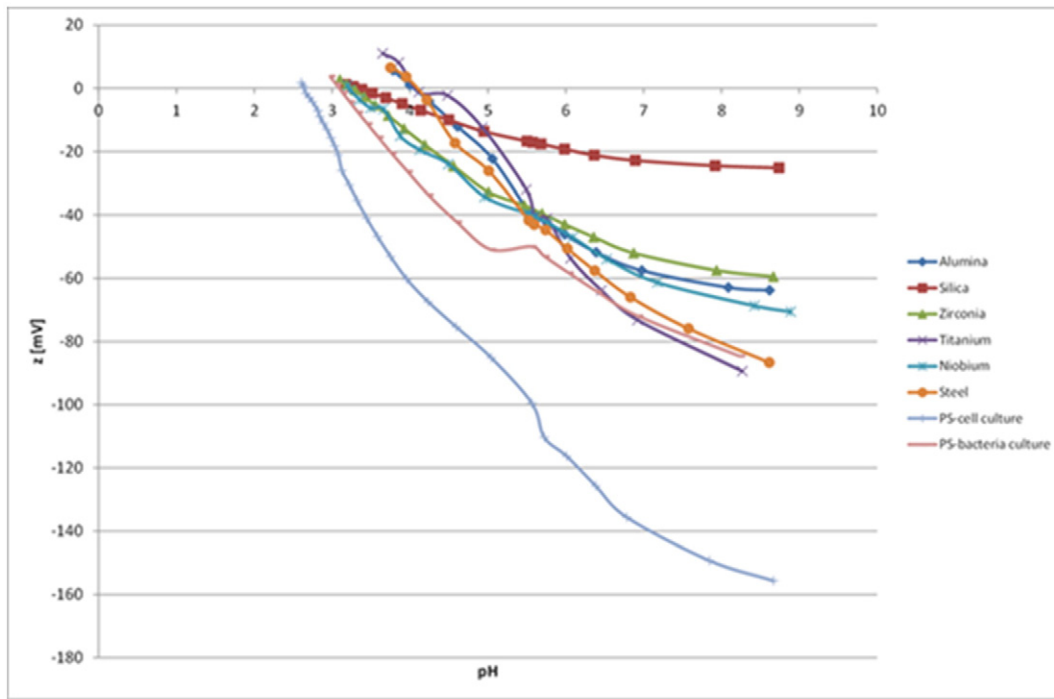


Fig. 5. Zeta potential vs pH for the selected materials.

and they are reported in the following. Polystyrene for cellular cultures shows the lowest isoelectric point (pH range = 2–3), while IEP values are similar for polystyrene for bacterial cultures, niobium, zirconia, alumina and silica (pH range = 3–4). Titanium and steel show an IEP slightly higher (pH range = 4–5).

As far as zeta potential is concerned, the curves of the different materials have different slope vs pH. All the considered materials are negatively charged at physiological pH (pH = 7.4), but the order of the tested materials respect to zeta potential is different respect to the IEP values. Polystyrene for cell cultures exhibits the highest negative zeta potential (average value of  $-150 \pm 10$  mV), silica the lowest (average value =  $-24 \pm 15$  mV). All the other materials present average values of zeta potential in the range between  $-50$  and  $-80$  mV at pH 7.4.

3.4. Protein adsorption

Fig. 6 reports the results of total protein adsorption on the selected materials (Fig. 6a) and western blot analysis of the absorbed proteins (Fig. 6b). It can be observed that alumina (group a – Fig. 6a) has the

highest total protein adsorption and silica (group c – Fig. 6a) the lowest (3 times lower than alumina). The other materials presented similar intermediate results without any statistical difference ( $p < 0.01$ ). Concerning western blot analysis, no selective adsorption of albumin, fibronectin or collagen has been evidenced for the tested materials, except silica where a lower amount of adhesive proteins (collagen and fibronectin) is detected.

3.5. Bacterial adhesion

The amount and viability of *S. aureus* colonies on the selected materials are reported in Fig. 7. The highest bacterial contamination (in terms of CFU counts) has been observed on both polystyrene surfaces (group a – Fig. 7) which are statistically different from all the other samples ( $p < 0.001$ ). Steel is in mid position (group b – Fig. 7) without any statistical difference respect to the other groups. All the other materials present a statistical difference respect to polystyrene surfaces (group c – Fig. 7 –  $p < 0.001$ ), while there is no significant difference within the group. The value of CFU of *S. aureus* biofilm on alumina has a greater

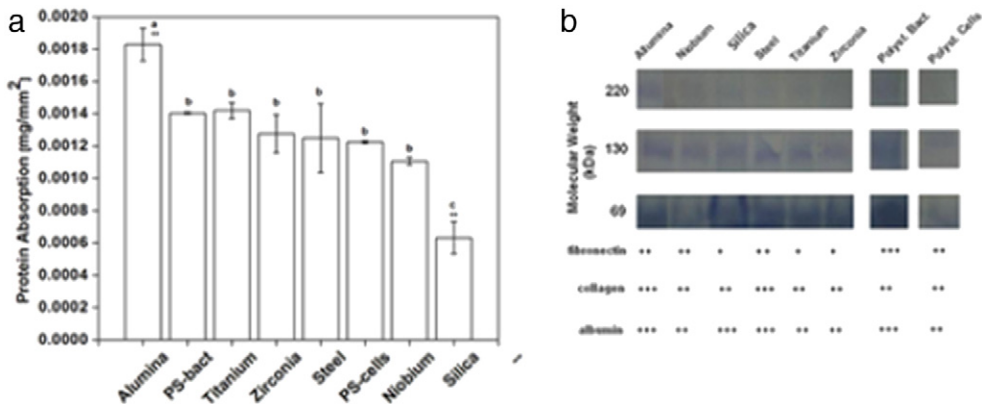


Fig. 6. Protein adsorption measurements. a) BCA quantification, b) western blot analyses.

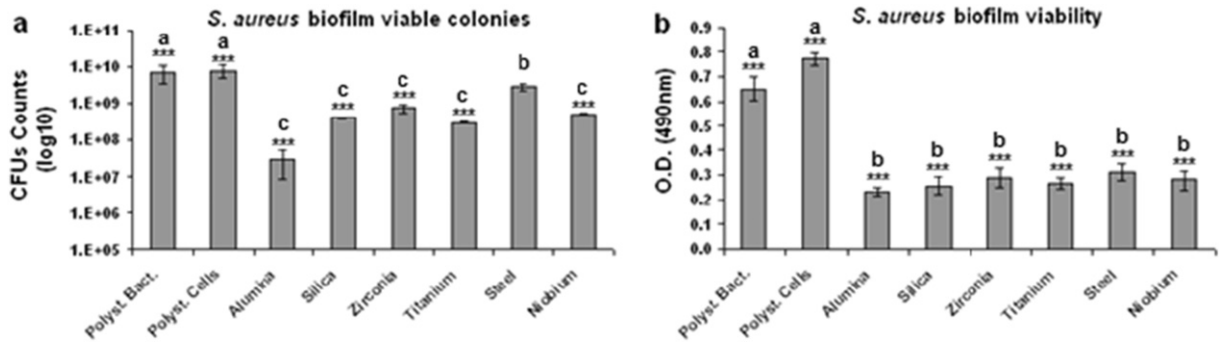


Fig. 7. Bacterial adhesion. a) Biofilm CFU count, b) biofilm viability (XTT).

statistical difference respect to polystyrene surfaces than the other samples of the group c ( $p < 0.0001$ ).

Concerning *S. aureus* biofilm viability, we can divide the tested materials into two groups: there is a significantly higher viability on both PS substrates and lower on the explored oxides and metals (slightly higher on steel).

### 3.6. Cell adhesion

Osteoblast cells viability and morphology on the selected materials are reported in Fig. 8. All the considered materials resulted as suitable for cells adhesion and spread with the only exception of polystyrene for bacteria culture (as expected considering the lack of surface treatment). A statistically higher cell viability was measured on polystyrene for cell culture (group a – Fig. 8a –  $p < 0.001$ ), the lowest on polystyrene for bacteria culture (group c – Fig. 8a), while all the other samples are in the same statistical group (group b – Fig. 8a).

Finally, SEM observations (Fig. 8b) of the materials of interest confirmed a comparable adhesion and spread of osteoblasts with the development of numerous filopodia on all the substrates of group b.

## 4. Discussion

As first, a detailed protocol for the preparation of the surfaces was developed. This procedure was selected in order to compare the behaviour of the different materials independently from the roughness effects, which are not the focus of the present research work. The proposed preparation protocol leads to smooth surfaces with comparable roughness values (0.007–0.04  $\mu\text{m}$ ) and good cleaning degree on all the tested materials, as confirmed by the profilometry and XPS analyses. No specific topography can be detected on the surfaces by means of SEM observation, despite some pores or few polishing tracks. The obtained

roughness range is below the critical threshold indicated in the literature for the increase of bacterial adhesion (0.2  $\mu\text{m}$ ) [62,63] and it can be supposed that it does not affect significantly cell/bacteria behaviour.

For a better comparison of the data, a sort of meta-analysis was performed and it is reported in Table 7. A progressive number from 1 to 6 was assigned to each surface for the different tests, considering that 1 was assigned to the surface with the lowest value in that test, 6 to the surface with the highest value and the surfaces with mid properties show a number in the range 2–5 proportional to the obtained value in that test.

As far as hydroxylation degree is concerned, different data were obtained by means of FTIR and XPS measurements, because of different penetration depth of these techniques and the different analysed sub-surface volume, as already observed by the authors [15,64]. XPS (lower penetration depth – in the range of few nanometers) detected an OH signal on all the investigated metals and oxides, with an increasing surface hydroxylation degree from titanium and alumina to zirconia and niobium, silica and finally steel. On the other side, no signal of hydroxyl group was detected through FTIR (higher penetration depth – in the range of some microns) on the investigated oxides, suggesting that the hydroxylated layer is thicker on the metals and thinner on the oxides. Absence of differences between the FTIR spectra of polystyrene for bacteria and cells culture can also be ascribed to the higher penetration depth of this technique. According to the literature, a zero hydroxylation degree was considered for untreated polystyrene for bacteria culture and a value equal to 10% for corona treated polystyrene for cell culture [34–36]. Considering that biological response is due to the outermost surface layer, we can conclude that XPS results are the most significant for the present analysis and they were considered in Table 7.

Concerning the wettability tests, the highest wettability by pure water has been observed for steel and the lowest for alumina and PS

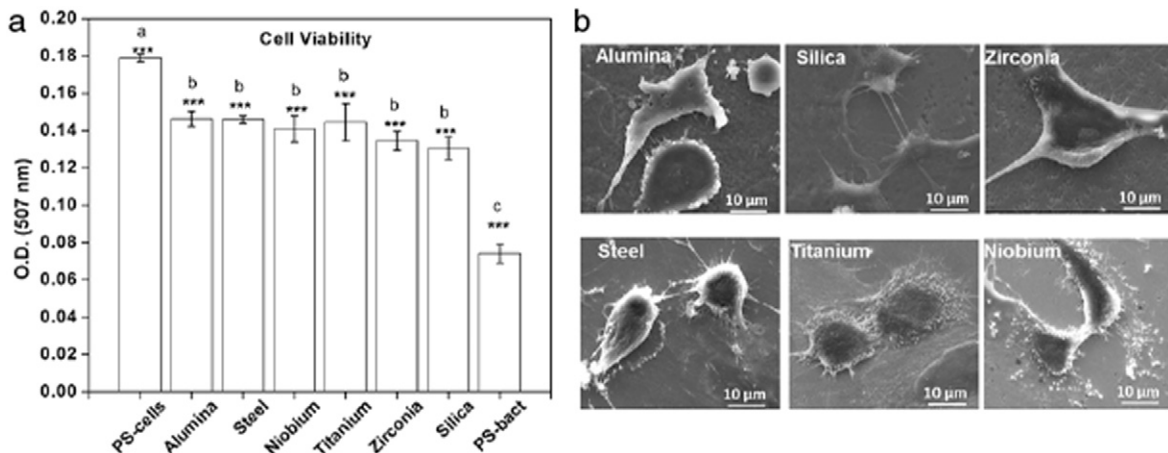


Fig. 8. Cell adhesion. a) Cell viability (MTT), b) cell morphology (SEM, group b).

for bacterial culture. These results are in accordance with the hydroxylation degree (except titanium), in fact a higher amount of OH groups can be associated with a higher wettability of the surface by polar liquids [65]. The rigorous surface cleaning protocol for all the tested materials (acetone and water washings followed by UV irradiation) allows the elimination of organic contaminants (always present onto reactive surfaces) and a consequent reliable correlation of wettability results with the hydroxylation degree, as suggested in [65]. These results confirm that the outermost surface layer is the most significant in order to determine the wetting behaviour of a material, as indicated by XPS results on surface hydroxylation, and suggest that hydroxylation degree is a key factor when the wetting liquid is pure water.

Considering the values of surface tension of the liquids used for testing, it is consistent to find values of contact angle not too far for water, SBF and bacteria/cells culture broths on several materials, considering that these liquids have comparable surface tension. In any case, the use of different liquids and media for wettability tests allows evidencing some unexpected differences such as between alumina and PS bact, which are similar and hydrophobic respect to several liquids, but show different behaviour when wetted by cell culture medium and FBS. Steel shows a quite different wetting behaviour by changing the liquid in the test.

Comparing the wettability data obtained on the same surface by changing the liquid from water to an inorganic saline solution (SBF), a consistent increase in wettability is registered on silica and PS-cell, while steel shows a consistent decrease. This effect can be related to a different ion adsorption from the examined surfaces.

The protein containing liquids (FBS, cell culture medium and bacterial broth) have a wetting behaviour not too far from SBF saline solution, with few exceptions: a bit higher wettability of alumina, zirconia and steel by cell culture medium.

Concerning measurement of wettability by blood, it can be considered a good simulation of *in vivo* behaviour, even if several factors must be considered for a correct interpretation of the data. Test temperature was 22 °C and not 37 °C, EDTA, used to prevent blood coagulation in this study, slightly increases blood density, viscosity and surface tension of blood. This can cause a slight increase in the sizes of blood drops, formation of longer blood ligaments and, consequently, more spherical droplets [66]. Even the inhomogeneity of the particles within the drops of blood and their adhesion with the substrates of the samples should be considered.

It is interesting to note that wettability by blood cannot be easily predicted by any other wettability test in a different fluid. This is consistent with the blood nature. Blood is a biological tissue in the fluid state, which consists of a continuous aqueous phase, plasma, containing many inorganic molecules and about 8% by weight of proteins (major among them fibrinogen, globulin and albumin), and the so-called figured elements (erythrocytes, leukocytes, platelets and chylomicrons) [67]. It can be concluded that if blood wetting is a key factor for biological response of a surface, specific tests must be performed.

Concerning the surface energy of the different tested materials, a general rule is that wettability increases if the surface energy increases, but this simple rule is not useful if comparison is performed on a wide range of materials as in this research.

Evaluation of the isoelectric point (IEP) by means of contact angle titration did not give reliable results. In fact, high data dispersion and a not univocal value for the IEP have been observed both for the one liquid and two liquids approaches.

On the other side, electrokinetic measurements gave reproducible and reasonable results, so this technique can be considered suitable for the measurement of the isoelectric point and zeta potential of bulk biomaterials. The isoelectric points of all the tested materials are comprised in the 2–5 pH interval and consequently all the tested materials are negatively charged at physiological pH (i.e. pH = 7.4). The lowest values for the isoelectric point have been registered for PS for cells and the highest ones for steel and titanium. These results are in

accordance with literature on titanium and silica [65,68,69], but not for the other tested materials [68,69], such as alumina and zirconia. This apparent inconsistency can be explained considering that most of the IEP and zeta potential measurements reported in literature are related to powder samples and surface charge of materials in bulk form can be substantially different because of the effects of sintering. Moreover, the technique used for both sample preparation and measurement are not always completely described and comparable. This point highlights the need of a systematic study of zeta potential of various materials in the same conditions in order to obtain comparable results. Measurements limited to IEP are useful in order to predict the sign of the surface charge, but not for a prediction of relative values of zeta potential at a specific pH of different materials.

As far as zeta potential at physiological pH is concerned, its magnitude on the different tested materials is different: the most negative one has been obtained on PS for cell cultures and the opposite on silica. This is the result of a balance among the different functional groups and ions present on the surface. The slope of the curves in the basic pH side of the graph makes also clear that only silica, showing an evident plateau, has only one type of functional group exposed on the surface (OH) [30]. It is evident that CORONA treatment on polystyrene is able to activate the surface and modify the zeta potential through a number of different functional groups: no plateau is evident in the zeta potential curve and a shift toward much more negative value is observed. When a surface treatment specifically increase the exposition of one functional group a plateau and a shift toward less negative values are observable in the zeta potential curves.

Meta-analysis reported in Table 7 shows that there is not a direct relationship between the trend of surface hydroxylation and that of zeta potential: no general rule can be found and zeta potential and surface charge are a much more complex effect than just a consequence of the presence of OH groups on the surface.

It is worth making a specific discussion on polystyrene. The material for bacteria culture is untreated, while that one for cell culture was CORONA treated. It is reported [70] that this process, as well as different plasma surface treatment, generates highly energetic oxygen ions which oxidize and graft onto the surface polystyrene chains, so that the surface becomes hydrophilic and negatively charged once medium is added. The data reported in Table 5 refer to experimental and literature data [34–36]. The increment of hydroxylation degree due to the CORONA treatment is low and consequently wettability by water, while it induces a consistent change in zeta potential and wettability by SBF and cell or bacteria broths.

The highest total protein adsorption has been observed on alumina and the lowest one on silica, while the other materials present an intermediate analogous behaviour. Interestingly, alumina and silica are substrates with respectively very low and high wettability. This result is in accordance with the literature consensus on a preferential protein adsorption (except for glycoproteins) on hydrophobic substrates compared to hydrophilic ones [71,72]. This phenomenon is explained considering that highly hydrophilic surfaces creates hydrogen bonds with the water molecules in the first steps of surface-fluid interaction (hydration) and that proteins, in order to be adsorbed onto the surface, must displace water molecules, with a certain energy consumption. The reduced protein adsorption on hydrophilic surfaces has been exploited in the realization of super-hydrophilic anti-adhesive and anti-fouling materials [73]. On the other hand, protein adsorption on surface charged materials can be induced by electrostatic interaction between the surface and the protein [74]. At the end, we observe the lowest adsorption on the surface presenting at the mean time high wettability, exposition of only one type of functional group (OH) and very low surface charge (silica), while in order to get a very high adsorption of proteins low wettability in both water based and protein containing media and a moderate surface charge are requested (alumina). Moreover, it must be considered that proteins can assume different configurations upon adsorption on hydrophilic/hydrophobic surfaces. It has been

reported that fibronectin shows a marked reduction in its cell-adhesive activity if adsorbed onto hydrophobic substrates, while its cell-stimulating functionality is maintained if adsorbed on hydrophilic ones [17].

As far as adsorption of specific proteins (albumin, fibronectin and collagen) is concerned, no defined trend has been observed on the investigated materials. Only a moderate decrease in the adsorption of adhesive proteins (collagen and fibronectin) can be underlined on silica substrates.

Concerning protein adsorption, interestingly no statistical difference among polystyrene for cells (CORONA treated) and bacteria (untreated) cultures was detected. It is reported [75] that the hydrophobic polystyrene surface must be modified to a more hydrophilic surface in order to maximise fibronectin adsorption providing a better surface for cells to attach, but this is not what we observed.

The highest bacterial contamination and biofilm viability has been observed on both polystyrene surfaces, with greater statistical difference with respect to alumina than the other samples. No relationship between surface charge or protein adsorption, bacterial adhesion and viability can be deduced from our data. A lower adhesion on the surface with the highest negative surface charge could be expected considering the negative surface charge of the used bacteria, as often reported as a general rule [76], but this behaviour is not evident in the present research. On the other side, it is reported that bacteria can use cell-adhesive proteins as preferential adhesion sites [77–79], but this expected trend is not congruent with our research. It appears from our results that a high Lewis acid (donor) component of the surface energy is able to increase bacterial adhesion according to the presence of a high Lewis basic (acceptor) component of the surface energy of bacteria [80]: it is difficult to say if this can be used as a general rule on different strains and different materials, but further work in this direction might be worthwhile.

All the considered materials resulted biocompatible and adherent substrates for osteoblast cells, except polystyrene for bacteria culture, as expected; moreover, statistically higher cell viability was measured on polystyrene for cell culture. It can be concluded that low hydroxylation degree, joined to low wettability both in SBF and in culture media results in a low cell adhesion, while surface treatment (such as CORONA) able to increase wettability in culture media and SBF, as well as to increase the amount of negative surface charge strongly increment cell adhesion. The case of silica shows that low protein and fibronectin adsorption alone is not able to inhibit cell adhesion on a strongly hydrophilic substrate. On the other side, a negative surface zeta potential (such as  $-150$  mV on polystyrene for cell culture) can be the decisive factor in order to increase cell viability. This effect is not due to a higher amount of adsorbed proteins, but probably to a higher activity of adhesion proteins such as fibronectin, as reported in [81].

An often reported general rule is that the polar component of surface energy has a great influence on cell adhesion on a biomaterial, with an increasing trend of cell attachment if the polar component increases. Our results show that the Lewis acid and basic component of the polar surface energy must be separately considered. The high Lewis basic component of the surface energy must be taken into account as a factor able to significantly reduce the cell viability as observed on PS bact.

It is often reported a general rule [82] about a threshold between adhesive and not adhesive surfaces at the critical surface tension of  $40$  mN/m (aqueous contact angle around  $60^\circ$ ), whereby surface with lower surface tension are not adhesive even if they show great protein adsorption. Our results compliant with the rule, but only if it is considered as a rough threshold value: it is not useful in order to qualitatively predict a progressive adhesion trend on different materials.

## 5. Conclusions

In conclusion, a systematic investigation of surface features and their relationships with biological response was performed on a wide range of biomaterials: oxides, metals and polymers. Some techniques were

found not useful at this aim, such as FTIR for measurement of hydroxylation degree and contact angle titration for evaluation of the isoelectric point (IEP).

An increment of surface hydroxylation degree was detected by means of XPS moving from titanium and alumina to zirconia or niobium, silica and finally steel. There is accordance between wettability data in water and the hydroxylation degree: a higher amount of OH groups can be associated with a higher wettability of the surface with polar liquids (steel) and vice versa (alumina). SBF, cells culture broths show values of surface tension not too far from water and consequently almost similar wettability behaviour on the tested surfaces, but some differences among look-alike materials can be evidenced by using different media in wetting tests. Wettability by blood cannot be easily predicted as a general rule by any other wettability test in different fluids. This is consistent with the completely different blood nature.

Concerning IEP, it must be directly measured on bulk specimens and cannot be easily assumed from data obtained on the same material in powder shape. Moreover, even if IEP measurements can predict the sign of a surface at different pH, the magnitude of the zeta potential must be directly measured by electrokinetic techniques. In our case, the highest negative zeta potential has been measured on PS for cell cultures and the lowest on silica. Zeta potential measurements are also useful in order to evidence the presence of one or more functional groups on the surface.

There is not a direct relationship between the trend of surface hydroxylation and that of zeta potential, because surface charge is a much more complex effect.

Concerning protein adsorption, we observe the lowest adsorption on the surface presenting at the mean time high wettability, the presence of only OH groups and very low surface charge (silica), while in order to get a very high adsorption of proteins low wettability in both water based and protein containing media and a moderate surface charge are requested (alumina): this observation join together two general rules on surface charge/hydrophilicity and protein adsorption often reported. No significant difference in protein adsorption was detected on polystyrene for cells and bacteria cultures.

The highest bacterial contamination and biofilm viability has been observed on both polystyrene surfaces: no relationship between surface charge or protein adsorption and bacterial adhesion and viability can be deduced from our data, while the presence of a high acid component of the surface energy seems to make the difference.

Concerning cell viability, it can be concluded that low hydroxylation degree, joined to low wettability both in SBF and in culture media results in low cell adhesion (PS-bact), while a negative surface zeta potential joined to a high polar component of surface energy can be the decisive factors in order to increase cell viability. The presence of a sort of rough threshold between adhesive and not adhesive surfaces at the critical surface tension of  $40$  mN/m is confirmed.

## Acknowledgements

EU Commission is acknowledged for the financial assistance (HERI-TAGE Erasmus Mundus Action 2 project Post-Doctoral Fellowship).

Ministry of Education, University and Research (M.I.U.R.-Italy) is kindly acknowledged for funding (PRIN 2010–2011 code 20102ZLNJ5\_006).

Anton Paar is acknowledged for its collaboration for zeta potential measurements and helpful discussion.

Sweden&Martina is kindly acknowledged for zirconia providing.

## References

- [1] B. Kasemo, *Biological Surface Science*, Surf. Sci. 500 (2002) 656.
- [2] P. Tengvall, in: D.M. Brunette, P. Tengvall, M. Textor, P. Thomsen (Eds.), *Titanium in Medicine*, Springer-Verlag, Berlin Heidelberg New York 2001, pp. 457–483.
- [3] D.M. Brunette, in: D.M. Brunette, P. Tengvall, M. Textor, P. Thomsen (Eds.), *Titanium in Medicine*, Springer-Verlag, Berlin Heidelberg New York 2001, pp. 485–512.



- [4] R.A. Latour Jr., in: G.E. Wnek, G.L. Bowlin (Eds.), *Encyclopedia of Biomaterials and Biomedical Engineering*, second ed. 2014, pp. 270–275.
- [5] A. Chaubey, K.J.L. Burg, in: G.E. Wnek, G.L. Bowlin (Eds.), *Encyclopedia of Biomaterials and Biomedical Engineering*, second ed. 2014, pp. 568–572.
- [6] A. Gristina, Biomaterial-centered infection: microbial adhesion versus tissue integration, *Science* 237 (1987) 1588.
- [7] B.D. Boyan, T.W. Hummert, D.D. Dean, Z. Schwartz, Role of material surfaces in regulating bone and cartilage response, *Biomaterials* 17 (1996) 137.
- [8] P.Y. Wang, W.T. Li, J. Yu, W.B. Tsai, Modulation of osteogenic, adipogenic and myogenic differentiation of mesenchymal stem cells by submicron grooved topography, *J. Mater. Sci. Mater. Med.* 23 (2012) 3015.
- [9] A. Zareidoost, M. Yousefpour, B. Ghaseme, A. Amanzadeh, The relationship of surface roughness and cell response of chemical surface modification of titanium, *J. Mater. Sci. Mater. Med.* 23 (2012) 1479.
- [10] P. Tambasco de Oliveira, S.F. Zalzal, M.M. Beloti, A.L. Rosa, A. Nanci, Enhancement of in vitro osteogenesis on titanium by chemically produced nanotopography, *J. Biomed. Mater. Res.* 80A (2007) 554.
- [11] S.D. Puckett, E. Taylor, T. Raimondo, T.J. Webster, The relationship between the nanostructure of titanium surfaces and bacterial attachment, *Biomaterials* 31 (2010) 706.
- [12] F. Vetrone, F. Variola, P. Tambasco de Oliveira, S.F. Zalzal, J.H. Yi, J. Sam, K.F. Bombonato-Prado, A. Sarkissian, D.F. Perepichka, J.D. Wuest, F. Rosei, A. Nanci, Nanoscale oxidative patterning of metallic surfaces to modulate cell activity and fate, *Nano Lett.* 9 (2009) 659.
- [13] K. Anselme, P. Davidson, A.M. Pupa, M. Giazzon, M. Liley, L. Ploux, The interaction of cells and bacteria with surfaces structured at the nanometre scale, *Acta Biomater.* 6 (2010) 3824.
- [14] S. Spriano, S. Ferraris, G. Pan, C. Cassinelli, E. Vernè, Multifunctional titanium: surface modification process and biological response, *J. Mech. Med. Biol.* 15 (2015) 1540001.
- [15] S. Ferraris, A. Venturello, M. Miola, A. Cochis, L. Rimondini, S. Spriano, Antibacterial and bioactive nanostructured titanium surfaces for bone integration, *Appl. Surf. Sci.* 311 (2014) 279.
- [16] F. Rupp, R.A. Gittens, L. Scheideler, A. Marmur, B.D. Boyan, Z. Schwartz, J. Geis-Gerstorfer, A review on the wettability of dental implant surface I: theoretical and experimental aspects, *Acta Biomater.* 10 (2014) 2894.
- [17] R.A. Gittens, L. Scheideler, F. Rupp, S.L. Hyzy, J. Geis-Gerstorfer, Z. Schwartz, B.D. Boyan, A review on the wettability of dental implants surfaces II: biological and clinical aspects, *Acta Biomater.* 10 (2014) 2907.
- [18] G. Zhao, Z. Schwartz, M. Wieland, F. Rupp, J. Geis-Gerstorfer, D.L. Cochran, B.D. Boyan, High surface energy enhances cell response to titanium substrate microstructure, *J. Biomed. Mater. Res.* 74A (2005) 49.
- [19] D. Kubies, L. Himmlova, T. Riedel, E. Chanova, K. Balik, M. Douderova, J. Bartova, V. Pesakova, The interaction of osteoblasts with bone implant materials: 1. The effect of physicochemical surface properties of implant materials, *Physiol. Res.* 60 (2011) 95.
- [20] C.I. Pereni, Q. Zhao, Y. Liu, E. Abel, Surface free energy effect on bacterial retention, *Colloid Surface B* 48 (2006) 143.
- [21] Y. Liu, Q. Zhao, Influence of surface energy of modified surfaces on bacterial adhesion, *Biophys. Chem.* 117 (2005) 39.
- [22] F. Schwarz, M. Wieland, Z. Schwartz, G. Zhao, F. Rupp, J. Geis-Gerstorfer, A. Schedle, N. Brogini, M.M. Bornstein, D. Buser, S.J. Ferguson, J. Becker, B.D. Boyan, D.L. Cochran, Potential of chemically modified hydrophilic surface characteristics to support tissue integration of titanium dental implants, *J. Biomed. Mater. Res. B* 88B (2009) 544.
- [23] M. Gasik, L. Van Mellaert, D. Pierron, A. Braem, D. Hofmans, E. De Waelheyns, J. Anné, M.F. Harmand, J. Vleugels, Reduction of biofilm infection risks and promotion of osteointegration for optimized surfaces of titanium implants, *Adv. Healthcare Mater.* 1 (2012) 117.
- [24] T. Kokubo, H. Takadama, How useful is SBF in predicting in vivo bone bioactivity, *Biomaterials* 27 (2006) 2907.
- [25] A.M. Visco, G. Galtieri, L. Torrisi, C. Scolaro, Properties of single and double lap polymeric joints welded by a diode laser, *Int. J. Polym. Anal. Ch.* 20 (2015) 442.
- [26] F. Caridi, A. Picciotto, L. Vanzetti, E. Iacob, C. Scolaro, Surface wet-ability modification of thin PECVD silicon nitride layers by 40 keV argon ion treatments, *Radiat. Phys. Chem.* 115 (2015) 49.
- [27] L. Liggieri, A. Passerone, An automatic technique for measuring the surface tension of liquid metals, *High Temp. Technol.* 7 (1989) 82.
- [28] E. McCafferty, J.P. Wightman, Determination of the surface isoelectric point of oxide films on metals by contact angle titration, *J. Colloid Interface Sci.* 194 (1997) 344.
- [29] D. Chedov, E.L.B. Logan, Surface charge properties of oxides and hydroxides formed on metal substrates determined by contact angle titration, *Colloids Surf. A Physicochem. Eng. Asp.* 240 (2004) 211.
- [30] T. Luxbacher, *The ZETA Guide: Principles of the Streaming Potential Technique*, Anton Paar, Austria, 2014.
- [31] J.M. Walker, The bicinchoninic acid (BCA) assay for protein quantitation, *The Protein Protocols Handbook*, Humana Press 2002, pp. 11–14.
- [32] A. Cochis, L. Fracchia, M.G. Martiniotti, L. Rimondini, Biosurfactants prevent in vitro *Candida albicans* biofilm formation on resins and silicon materials for prosthetic devices, *Oral Surg. Oral Med. Oral Pathol. Oral Radiol.* 113 (2012) 755.
- [33] A. Cochis, B. Azzimonti, C. Della Valle, R. Chiesa, C.R. Arciola, L. Rimondini, Biofilm formation on titanium implants counteracted by grafting gallium and silver ions, *J. Biomed. Mater. Res. A* 103 (2015) 1176.
- [34] B. Fryer, S. Nelson, V. Nielsen, T. Brevig, T.K. Marwood, *Methods, Surface Modified Plates and Compositions for Cell Attachment, Cultivation and Detachment*, WO2009105570 A2, 2009.
- [35] A. Carré, K.L. Mittal, *Surface and Interfacial Aspects of Cell Adhesion*, Ed. EIDEN, Boston, 2010 454–456.
- [36] J. Granchelli, *Biotech International*, <http://www.biotech-online.com/featured-articles/surface-innovation-optimising-cell-adhesion/index.html> 2009 (7th June 2016, 10:44 a.m.).
- [37] H. Habazaki, M. Yamasaki, T. Ogasawara, K. Fushimi, H. Konno, K. Shimizu, T. Izumi, R. Matsuoka, P. Skeldon, G.E. Thompson, Thermal degradation of anodic niobia on niobium and oxygen-containing niobium, *Thin Solid Films* 516 (2008) 991.
- [38] <http://srdata.nist.gov/xps/> (28 April 2015, 16:54).
- [39] T. Hanawa, S. Hiromoto, A. Yamamoto, D. Kuroda, K. Asami, XPS characterization of the surface oxide film of 316L stainless steel samples that were located in quasi-biological environments, *Mater. Trans.* 43 (2002) 3088.
- [40] S. Ardizzone, C.L. Bianchi, Electrochemical features of zirconia polymorphs. The interplay between structure and surface OH species, *J. Electroanal. Chem.* 465 (1999) 136.
- [41] G. Lefevre, M. Duc, P. Lepeut, R. Caplain, M. Fedoroff, Hydration of alumina in water and its effects on surface reactivity, *Langmuir* 18 (2002) 7530.
- [42] E. Vernè, C. Vitale-Brovarone, E. Bui, C.L. Bianchi, A.R. Boccacini, Surface functionalization of bioactive glasses, *J. Biomed. Mater. Res.* 90A (2009) 981.
- [43] M. Textor, C. Sittig, V. Frauchiger, S. Tosatti, D.M. Brunette, in: D.M. Brunette, P. Tengvall, M. Textor, P. Thomsen (Eds.), *Titanium in Medicine*, Springer-Verlag, Berlin Heidelberg New York 2001, pp. 417–453.
- [44] E. Zhang, C. Zou, S. Zeng, In-vitro bioactivity, biocorrosion and antibacterial activity of silicon integrated hydroxyapatite/chitosan composite coating on 316 L stainless steel implants, *Surf. Coat. Technol.* 203 (2009) 1075.
- [45] M. Minella, M.G. Faga, V. Maurino, C. Minero, E. Pelizzetti, S. Coluccia, G. Martra, Effect of fluorination on the surface properties of titania P25 powder: an FTIR study, *Langmuir* 26 (4) (2010) 2521.
- [46] A. Balamurugan, G. Sockalingum, J. Michel, J. Fauré, V. Banchet, L. Wortham, S. Bouthors, D. Laurent-Maquin, G. Balossier, Synthesis and characterisation of sol gel derived bioactive glass for biomedical applications, *Mater. Lett.* 60 (2006) 3752.
- [47] Vasconcelos, E.H.M. Nunes, A.C.S. Sabioni, P.M.P. Vasconcelos, W.L. Vasconcelos, Optical characterization of 316L stainless steel coated with sol-gel titania, *J. Non-Cryst. Solids* 358 (2012) 3042.
- [48] A. Pawlicka, M. Atik, M.A. Aegerter, Synthesis of multicolor Nb2O5 coatings for electrochromic device, *Thin Solid Films* 301 (1997) 236.
- [49] C.P. Tripp, R.P.N. Veregin, M.L. Hair, Effect of fluoralkyl substituents on the reaction of alkylchlorosilanes with silica surfaces, *Langmuir* 9 (1993) 3518.
- [50] V.G. Prasanth, G. Prasad, T. Kiran, R.S. Rathore, M. Pathak, K.I. Sathyanarayanan, Synthesis, spectral characterization and crystal structure of a new precursor (CH<sub>3</sub>COCHCOCH<sub>3</sub>)<sub>2</sub>Zr(C<sub>6</sub>H<sub>4</sub>(N = CHC<sub>6</sub>H<sub>4</sub>O)<sub>2</sub>) for nano-zirconia: an investigation on the wettability of polyvinylidene fluoride-nano-zirconia composite material, *J. Sol-Gel Sci. Technol.* 76 (2015) 195.
- [51] S. Guruvenket, G. Mohan Rao, M. Komath, A.M. Raichur, Plasma surface modification of polystyrene and polyethylene, *Appl. Surf. Sci.* 236 (2004) 278.
- [52] C.J. van Oss, *Interfacial Forces in Aqueous Media*, second ed. CRC Press, Boca Raton, FL, 2006.
- [53] M. Amaral, M.A. Lopes, J.D. Santos, R.F. Silva, Wettability and surface charge of Si<sub>3</sub>N<sub>4</sub>-bioglass composites in contact with simulated physiological liquids, *Biomaterials* 23 (2002) 4123.
- [54] K. Yoshimura, L.C. Chen, D. Asakawa, K. Hiraoka, S. Takeda, Physical properties of the probe electrospray ionization (PESI) needle applied to the biological samples, *J. Mass Spectrom.* 44 (2009) 978.
- [55] L. Jiang, C. Shen, X. Long, G. Zhang, Q. Meng, Rhamnolipids elicit the same cytotoxic sensitivity between cancer cell and normal cell by reducing surface tension of culture medium, *Appl. Microbiol. Biotechnol.* 98 (2014) 10187.
- [56] *Enciclopedia Medica Italiana*, vol. 2, USES Edizioni Scientifiche Firenze, 1991.
- [57] C.J. Van Oss, R.J. Good, M.K. Chaudhury, Additive and nonadditive surface tension components and the interpretation of contact angles, *Langmuir* 4 (1988) 884.
- [58] E.M. Harnett, J. Alderman, T. Wood, The surface energy of various biomaterials coated with adhesion molecules used in cell culture, *Colloids Surf. B* 55 (2007) 90.
- [59] <http://www.surface-tension.de/solid-surface-energy.htm> (20th May 2016, 14:11).
- [60] [http://www.accudynetest.com/polytable\\_02.html?sortBy=sort\\_hansent](http://www.accudynetest.com/polytable_02.html?sortBy=sort_hansent) (20th May 2016, 14:12).
- [61] Y.-L. Ong, A. Razatos, G. Georgiou, M.M. Sharma, Adhesion forces between *E. coli* bacteria and biomaterial surfaces, *Langmuir* 15 (1999) 2719.
- [62] V. Frijd, P. Linderback, A. Wennerberg, L.C. de Paz, G. Svensater, J.R. Davies, Effect of nanoporous TiO<sub>2</sub> coating and anodized Ca<sup>2+</sup> modification of titanium surfaces on early microbial biofilm formation, *Oral Health* 11 (2011) 8.
- [63] M. Quirynen, C.M.L. Bollen, W. Papaioannou, J. Van Eldere, D. van Steenberghe, The influence of titanium abutment surface roughness on plaque accumulation and gingivitis: short term observations, *Int. J. Oral Maxillofac. Implants* 11 (1996) 169.
- [64] S. Ferraris, S. Spriano, G. Pan, A. Venturello, C.L. Bianchi, R. Chiesa, M.G. Faga, G. Maina, E. Vernè, Surface modification of Ti-6Al-4V alloy for biomineralization and specific biological response: part I, inorganic modification, *J. Mater. Sci. Mater. Med.* 22 (2011) 533.
- [65] A. Kanta, R. Sedev, R. Ralston, Thermally- and photo induced changes in the water wettability of low surface area silica and titania, *Langmuir* 21 (2005) 2400.
- [66] E. Hrnčíř, J. Rosina, Surface tension of blood, *Physiol. Res.* 46 (1997) 319.
- [67] M. Thieret, *Biology and Mechanics of Blood Flows – Part II: Mechanics and Medical Aspects*, Springer, New York, 2008.
- [68] B.S. Bal, M.N. Rahaman, Orthopedic applications of silicon nitride ceramics, *Acta Biomater.* 8 (2012) 2889.
- [69] M. Kosmulski, pH dependent surface charging and point of zero charge. IV. Update and new approach, *J. Colloid Interface Sci.* 337 (2009) 439.
- [70] <http://www.sigmaaldrich.com/technical-documents/articles/biofiles/evolution-of-cell.htm> (20th May 2016, 14:27).

- [71] M. Rabe, D. Verdes, S. Seeger, Understanding protein adsorption phenomena at solid surfaces, *Adv. Colloid Interfac.* 162 (2011) 87.
- [72] E.A. Vogler, Protein adsorption in three dimensions, *Biomaterials* 33 (2012) 1201.
- [73] S. Chen, L. Li, C. Zhao, J. Zheng, Surface hydration: principles and applications toward low-fouling/nonfouling biomaterials, *Polymer* 51 (2010) 5283.
- [74] P. Silva-Bermudez, S.E. Rodil, An overview of protein adsorption on metal oxide coatings for biomedical implants, *Surf. Coat. Technol.* 233 (2013) 147.
- [75] F. Grinnell, M.K. Feld, Fibronectin adsorption on hydrophilic and hydrophobic surfaces detected by antibody binding and analyzed during cell adhesion in serum-containing medium, *J. Biol. Chem.* 257 (1982) 4888.
- [76] M. Katsikogianni, Y.F. Missirlis, Concise review of mechanisms of bacterial adhesion to biomaterials and of techniques used in estimating bacteria-material interactions, *Eur. Cell Mater.* 8 (2004) 37.
- [77] K.M. Holgers, A. Ljungh, Cell surface characteristics of microbiological isolates from human percutaneous titanium implants in the head and neck, *Biomaterials* 20 (1999) 1319.
- [78] C.R. Hauck, F. Agerer, P. Muenzner, T. Schmitter, Cellular adhesion molecules as targets for bacterial infection, *Eur. J. Cell Biol.* 85 (2006) 235.
- [79] F.H. Jones, Teeth and bones: applications of surface science to dental materials and related biomaterials, *Surf. Sci. Rep.* 42 (2001) 75.
- [80] K.L. Mittal, *Acid-base Interactions: Relevance to Adhesion Science and Technology*, vol. 2, VSP, 1991.
- [81] B.E. Rapuano, D.E. MacDonald, Surface oxide net charge of a titanium alloy: modulation of fibronectin-activated attachment and spreading of osteogenic cells, *Colloid Surface B* 82 (2011) 95.
- [82] J.O. Hollinger, *An Introduction to Biomaterials*, CRC Press, Taylor & Francis Group, Boca Raton, FL, 2012.